Chapter 1
Laser Physics for Materials Scientists: A Primer

Richard F. Haglund

Abstract Laser processing of materials has achieved significant successes in pulsed laser deposition, micro- and nanostructuring and surface modification and analysis. However, materials scientists often do not think about the physics of those lasers, which determines their properties and therefore also the way in which these lasers can be employed in laser processing. This chapter discusses the essential theory of laser gain, oscillation and amplification, and provides examples drawn from lasers now frequently used in materials processing. The implications for the design of new lasers and new materials-processing strategies are considered, using the example of a picosecond laser system for polymer processing.

1.1 Introduction

To optimize laser processing for specific applications and materials, it is useful to understand how lasers function, not only to select the correct lasers for particular processes, but also to provide input to laser designers and builders for new developments. In the future, an increased understanding of laser-materials interactions as these relate to laser properties will feed back into the laser-building community, to enable materials scientists to play a role in:

- Designing and constructing broadly tunable laser systems, at reasonable cost, capable of being tuned to the parameters that optimize process throughput based on fundamental laser-matter interactions;
- Understanding how the choice of amplified versus oscillator-only laser systems enables or limits the application of lasers in new processing applications as well as efficiency and overall throughput; and

R. F. Haglund (✉)
Department of Physics and Astronomy, Vanderbilt University,
Nashville, TN 37235-1807, USA
e-mail: richard.haglund@Vanderbilt.Edu

M. Castillejo et al. (eds.), *Lasers in Materials Science*,
Springer Series in Materials Science 191, DOI: 10.1007/978-3-319-02898-9_1,

Table 1.1 Characteristics of lasers used in materials processing

Laser type	Pulse duration	Repetition frequency	Wavelength range (μm)	Fluence	Intensity
Fiber laser oscillators	CW-1 ps	CW-MHz	1.07–2.1	Modest	High
Amplified fiber lasers	Ns-fw	kHz-MHz	1.07–2.1	High	High
Diode lasers	CW-μs	CW-kHz	0.8–1.2	Modest	Low
Excimer oscillator	10–20 ns	200 Hz	0.308, 0.248, 0.193	High	Modest
Excimer amplifier	1–10 ps	10 Hz	0.248	High	High
Nd:YAG oscillators	5–20 ns	20 Hz	1.06, 0.532, 0.355, 0.266	High	Modest
Nd:YVO_4 oscillators	5–10 ns	20 kHz	1.06, 0.532, 0.355, 0.266	Modest	Low
Yb:YAG amplifiers	0.5–20 ps	20 MHz	1.06, 0.532, 0.355, 0.266	Modest	High
Ti:sapphire oscillator	10–100 fs	100 MHz	0.7–1.0	Low	High
Ti:sapphire amplifier	100–150 fs	5 kHz	0.7–1.0	High	High
Yb:YAG + OPA	10–100 ps	1–5 kHz	0.2–20	Modest	High

- Developing figures of merit that will enable comparisons among laser systems in selecting scalable tools for applications, such as thin-film deposition, where current laser processes are not competitive with conventional processing tools.

Meeting these challenges would not only enlarge the palette of materials that can be built, assembled and fabricated using the unique electronic and vibrational interactions of light with matter, but also expand the emphasis from bulk and thin-film processing to micro- and nanoscale materials modification where the incomparable precision of laser processing holds sway.

Lasers commonly used for processing advanced materials can be categorized according to their (1) temporal pulse structure; (2) laser frequency range; and (3) tradeoffs between intensity and fluence based on pulse energy and duration. The throughput or processing rate will, as will be shown later, depends on average power. Especially during the last decade, the number of different laser types used in materials processing has expanded significantly; commercially available laser systems cover a range of all these properties, as shown in Table 1.1.

Figure 1.1 illustrates the parameter space relevant to laser processing materials, spanned by laser pulse duration and laser intensity. Solid and dashed diagonal lines show contours of constant fluence. For example, the line 1 J/cm^2 is the line representing the threshold for many laser processes initiated by pulsed nanosecond lasers, as in pulsed laser deposition. Below the line representing a fluence of 10 mJ/cm^2, mesoscale atomic motion within a material is relatively unlikely; in this region, local phase changes and other subtle modifications to local materials properties can be achieved. Above the fluence of 100 J/cm^2, on the other hand,

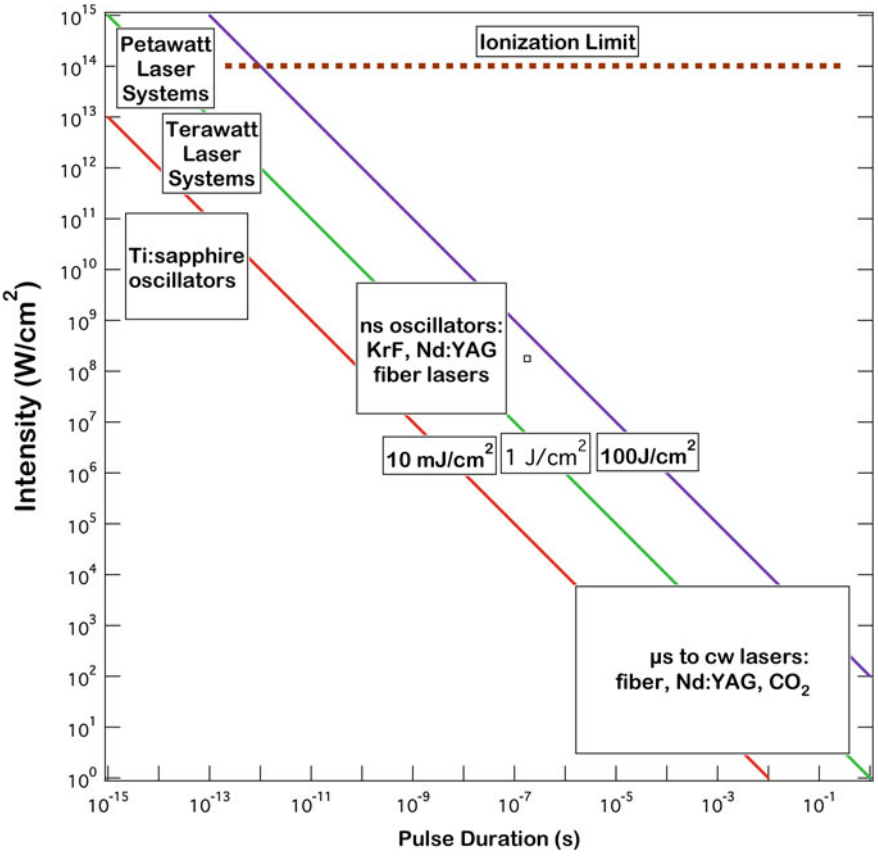

Fig. 1.1 A map of the parameter space occupied by current lasers used in materials processing. *Lines of constant fluence* are shown covering the range where most materials processing can occur

most materials modifications that are induced by lasers tend to be destructive for short- and ultrashort-pulse lasers, while at the limit of very long pulses, the changes tend to be thermal. As shown in Fig. 1.1, the laser systems listed in Table 1.1 nevertheless cover a wide range of the parameter space available for useful materials processing.

In this chapter, we first consider the fundamentals of laser interactions with materials as these relate to the choice of laser systems, and develop a simple figure-of-merit that makes it possible to see how various properties of a laser influence overall process throughput—and hence the economic merit of laser processing that can be compared to other processes. Next, we consider the fundamental theory of laser oscillators and amplifiers that are germanely to laser processing of materials, including ways of controlling laser pulse duration and repetition frequency. Finally, we present an example of a tunable, picosecond

mid-infrared laser system based on currently available oscillators, amplifiers and parametric generators, illustrating how considering laser physics and laser properties can drive new modes of materials processing.

1.2 Fundamentals of Laser-Materials Interactions

Materials modification by lasers requires the motion of atoms, ions or molecules—which of necessity requires complex interactions in the material since photons carry very little momentum. To achieve atomic motion, three conditions must, in general, be met: First, a threshold intensity is needed to initiate the process, generally a few $\mathrm{MW} \cdot \mathrm{cm}^{-2}$. Second, vibrational energy—whether generated directly by infrared photon absorption or by multi-phonon cascades following electronic excitation—must be localized on a small group of atoms or a molecular-size cluster in the laser-irradiated solid for longer than a few vibrational periods. Third, the energy absorbed must be sufficient to initiate and sustain the breaking of bonds and the mesoscale motion of atoms, ions, molecules and clusters. In laser ablation, for example, the ejection of mesoscale volumes of material also creates a dense plume in which the interactions of atoms, ions, molecules and clusters with each other and with the laser light play a significant role.

Efficiency in materials modification and processing is enhanced by attending to the *hierarchical* character of laser-materials interactions. The crucial roles played by localized temporal and spatial excitation density in materials processing were first adumbrated by Stoneham and Itoh [1] and Itoh and Stoneham [2]. Their fundamental concept of localized excitation density is central to the idea of selective or non-thermal materials processing ranging from the visible-ultraviolet to the "molecular fingerprint" regions of the electromagnetic spectrum. This perspective is based on an *atomic-* or *molecular-scale* photon-matter interactions that generate *mesoscale* effects on time scales that are short compared to thermal equilibration times. Ultimately, the development of resulting in *macroscale* materials modifications on micro- to millimeter length scales.

Figure 1.2 shows schematically the sequence of processes through which the initial absorption of laser photons ultimately leads to macroscopic effects, such as those found in laser ablation, laser cutting and multiphoton structuring. By choosing the laser pulse duration or scanning speed to illuminate the target volume for a duration shorter than the thermal confinement time [3]

$$\tau_{thermal} = L_p^2 \Big/ D_{thermal} \tag{1.1}$$

(where L_{opt} is the optical penetration depth and $D_{thermal}$ is the thermal diffusivity), which in many technologically important materials is typically 0.1–10 μs, energy deposition into thermal modes of the target can be confined and the creation of a heat-affected damage zone by diffusion largely avoided, provided of course that the desired processing effect also occurs on a shorter time scale. Analogously,

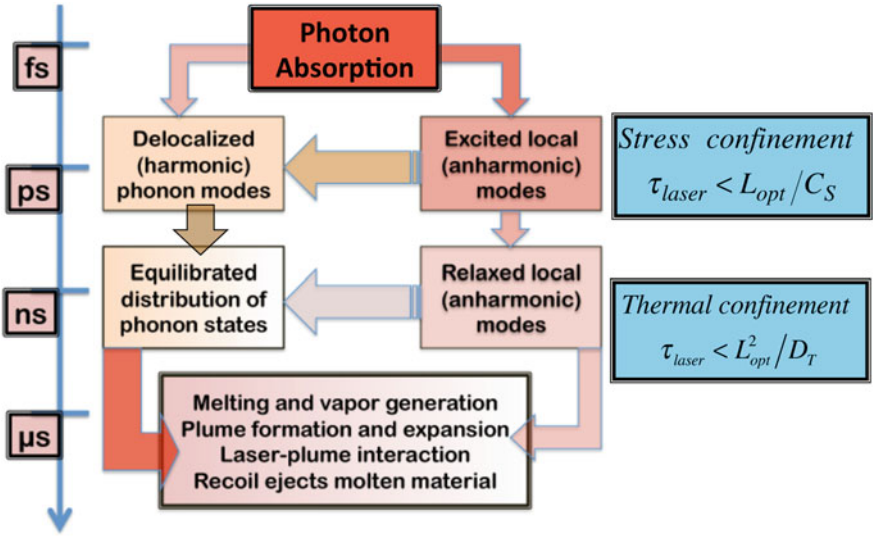

Fig. 1.2 Dynamics of photon absorption, electronic or vibrational excitation and relaxation processes leading to materials modifications such as ablation, melting and the formation of recoil-induced ejecta. The time scales relevant to stress confinement and thermal confinement are also shown

when the micropulse duration is shorter than the stress confinement time defined by [4–6]

$$\tau_{stress} = L_p / C_{sound} \tag{1.2}$$

(typically 001–0.1 μs), materials modification due to the propagation of photo-mechanically generated shock waves, spallation and exfoliation will likewise be limited to the volume in which the laser energy is absorbed.

When laser pulses excite a resonant electronic or vibrational mode of a solid, the persistence of the deposited energy in that mode and the specific relaxation mechanisms that relax or release the deposited energy determine whether or not a non-thermal process results from the laser excitation [7]. The time evolution of the laser-excited process follows from the basic quantum–mechanical result for the time rate of change of the yield of a particular process:

$$\frac{dN_0}{dt} = \eta N_0 \sigma_{(k)} \left(\frac{I}{\hbar\omega} \right)^k \tag{1.3}$$

where N_0 is the number of atoms or molecules per unit volume in the process volume, η is the quantum efficiency of the process, including loss channels; $\sigma_{(k)}$ the kth order cross section for the laser interaction with the material; and $\Phi = I/\hbar\omega$ is the photon flux, the number of photons per unit time per unit area.

From (1.3) it is evident that the rate at which a process occurs—critically important to the economics of materials processing—must then be proportional to average power. Since the probability for initiating nonlinear processes scales with powers of the intensity, rather than fluence, pulse durations of order a few picoseconds appear to have significant advantages for materials modification and processing. In particular, when the material is excited by ultrashort pulses, the initially spatially localized, anharmonic electronic or vibrational excitations are diluted only after enough time has elapsed for them to begin mixing with the delocalized, harmonic modes of the phonon bath *following* the laser pulse, whereas with nanosecond laser pulses, this relaxation begins already *during* the exciting laser pulse.

In choosing lasers for application to materials properties, it is useful to remember that the macroscopic observables—such as total yield—necessarily scale with energy deposited per unit volume (E/V):

$$Yield \propto \left(\frac{E}{V}\right) = F_L \alpha(\omega, I) \cong I_0 \tau_L [\alpha_0(\omega) + \beta \cdot I(z,t)] \tag{1.4}$$

where F_L is the laser fluence, α and β are the linear and nonlinear absorption coefficients, ω and I are the laser frequency and intensity, respectively, and z and t are the relevant space (penetration depth) and time coordinates.

The interplay of laser energy and intensity can be understood in a qualitative way by calculating the effective temperature reached in a given target volume, where the effective temperature is simply the proxy for the energy required to effect a particular materials modification. The temperature reached by absorption of a single laser pulse, the number of pulses and the rate at which they are delivered by the laser turn out to be key parameters for calculating the effect of the laser-materials interaction, assuming that the laser energy is ultimately converted into processes that eventually reach thermal equilibrium. From the analytical solution to the one-dimensional heat-conduction equation, the target temperature during a single laser pulse reaches an average value [8]

$$\langle T \rangle = \sqrt{\frac{2}{\pi}} \frac{I_{abs} \sqrt{a \cdot \tau_L}}{\kappa}, \quad a \equiv \frac{\kappa}{C_v \rho_0} \tag{1.5}$$

If all the absorbed energy is converted into the desired materials modification (e.g., vaporization, melting, annealing), then the specific energy input per unit volume is given by

$$\frac{E_{abs}}{V} = C_p \rho_0 \langle T \rangle = \rho_0 \Omega \tag{1.6}$$

where Ω is the binding energy per atom, another material-dependent parameter. Once thermal equilibrium is reached—typically in a few picoseconds—the temperature rise in the laser-irradiated volume as a function of laser and materials parameters can be computed as follows:

$$\Delta T = \frac{F_{abs}(\omega) \cdot \alpha(\omega, I)}{C_v \rho_0} = \frac{F_{abs}(\omega) \cdot [\alpha(\omega_0) + \beta I_{abs}]}{C_v \rho_0}, I_{abs} \tau^{1/2} = \sqrt{\frac{\pi a}{2} \Omega} \equiv f(a, \Omega) \tag{1.7}$$

The processing *rate Y*—for example, the rate of material removal in a laser ablation process leading to the deposition of a thin film—for a laser producing pulses at a rate N_{pps} with energy E_L per pulse is given by

$$Y = \eta(\omega, I) \left(\frac{E}{V} \right) N_{pps} \cong \eta(\omega, I) \frac{E_L f(a, \Omega)}{L_{opt} A(F_0, \omega)} N_{pps} \tag{1.8}$$

Here L_{opt} is the optical absorption length, $A(F_0, \omega)$ is the laser spot size at the material modification threshold for the given laser frequency, and F_0 is the threshold fluence.

From (1.8), the yield (in units of processing events per unit time) depends critically both on the materials parameters $f(a, \Omega)$ and L_{opt}, and on the pulse repetition frequency, whereas the specific energy deposition benefits from nonlinear effects in the target material. Hence, it becomes virtually axiomatic that the most efficient lasers for many materials processing protocols will be high-intensity (hence ultrashort pulse), high pulse-repetition frequency devices. Optimal laser processing conditions can be achieved by choosing short optical depth, small focal spots, and high pulse-repetition frequency to achieve efficient materials modification, as reflected in (1.8) that describes the overall processing rate.

1.3 Fundamentals of Laser Physics

The characteristics of the photon beam that emerges from the laser are determined by three essential components: the gain medium, the pump or excitation source, and the optical cavity. The abbreviated treatment here illustrates how the characteristics of all three contribute to the properties of the beam, and follows the general lines found in [9]; additional details can be found in [10–12].

1.3.1 Electromagnetic Waves in a Medium with Gain and Absorption

Consider an atomic, ionic or molecular system with two energy levels, E_1 and E_2, in thermal equilibrium. The relative population densities of the two levels N_1 and N_2 are given by Boltzmann's equation:

$$N_1 = N_0 \exp[-(E_1 - E_0)/k_B T], N_2 = N_0 \exp[-(E_2 - E_0)/k_B T] \\ \Rightarrow \frac{N_2}{N_1} = \exp[-(E_2 - E_1)/k_B T] \tag{1.9}$$

where k_B is the Boltzmann constant, T is the absolute temperature, and N_0 is the ground-state population density. When an electric field interacts with such a two-level atomic system, its evolution in space and time is expressed by

$$E(\omega, t) = E_0 \exp\{i[\omega t - k'(\omega)z]\} \tag{1.10}$$

The propagation constant is related to the susceptibility of the two-level medium by

$$k'(\omega) = k + k\frac{\chi'(\omega) + i\chi''(\omega)}{2n^2} - \frac{i\alpha}{2} = k + k\frac{\chi'(\omega)}{2n^2} + \frac{i\gamma(\omega)}{2} - \frac{i\alpha}{2} \tag{1.11}$$

where the vacuum wave number is k and α is the distributed loss. The optical gain or loss at the frequency ω is thus proportional to the imaginary part of the propagation constant; the sign of $\gamma(\omega)$ also depends only on the relative size of the populations in states N_1 and N_2.

$$\gamma(\omega) \equiv k\frac{i\chi''(\omega)}{n^2} = \left[N_2 - \left(\frac{g_2}{g_1}\right)N_1\right]\frac{\pi c^2 A_{21}}{2\omega^2} g(\omega_0, \omega) \tag{1.12}$$

As an electromagnetic wave propagates through a medium with a complex dielectric function, the change in intensity is related to the average power absorbed per unit volume by

$$\frac{dI}{dz} = -\frac{\overline{Power}}{Volume} = -\frac{\omega\varepsilon_0}{2}\chi''|E(\omega, z)|^2 = I_0 \exp\{[\gamma(\omega) - \alpha]z\} \tag{1.13}$$

Thus if the gain at any given frequency exceeds the distributed loss, the incoming wave with intensity I_0 will be amplified; if the loss dominates, an incoming electromagnetic wave will be attenuated. The key to making a successful laser oscillator or amplifier is therefore to create a population inversion that makes the factor in braces in (1.13) positive; the second is to reduce the distributed losses α due to scattering, reflection and absorption in the laser medium and the optical resonator to a minimum.

1.3.2 Creating Gain in a Laser Medium

In any system of atoms, ions or molecules in thermal equilibrium, the population in state 2 is always exponentially less than that in state 1. Hence, creating gain, rather than loss, in a laser medium requires the creation of a highly non-equilibrium distribution of atoms. This is the function of the laser "pump," which may be

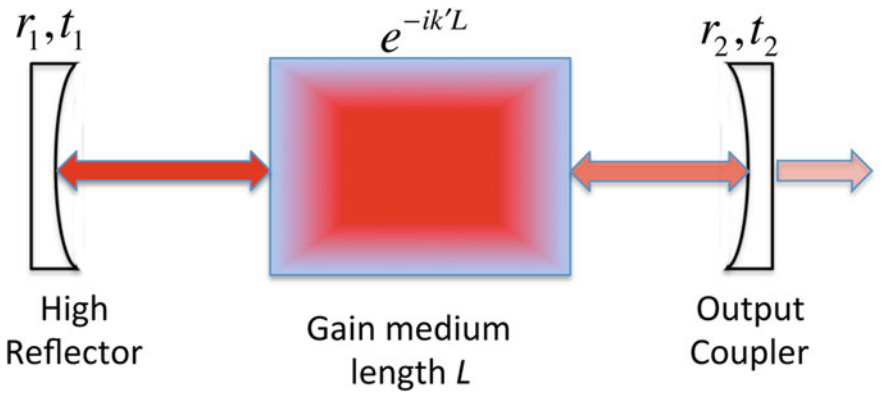

Fig. 1.3 Schematic of a Fabry–Perot resonator, showing how phase and amplitude accumulate with increasing numbers of round trips through the cavity

a flashlamp, an electron beam, an electric discharge, an electric current or even another laser. While flashlamps and electric discharges are still used in many nanosecond laser oscillators, the development of high-efficiency laser diodes operating in the near infrared has made optical pumping an increasingly popular choice, especially for mode-locked and fiber lasers, because of the uniformity and stability of their output and the efficiency with which the diode lasers can be coupled directly into the desired pump transition.

1.3.3 Laser Oscillators: Theory

The possibility of light amplification by stimulated emission leads naturally to the question of how to build an oscillator—that is, an optical device in which a very small input signal can grow into a self-sustaining optical beam, either continuous or pulsed. Such an oscillator may be either pulsed or continuous-wave (CW); regardless of which it is, the basic principles remain the same. As a model system (Fig. 1.3), we consider a simple laser cavity with a gain medium of length L, which is essentially a pair of resonator mirrors that are perfectly aligned. For the sake of definiteness, we assume that one mirror is a high reflector, with reflection and transmission coefficients (r_1, t_1), while the other mirror, the output coupler, is partially transmitting with coefficients (r_2, t_2). If we imagine the initially infinitesimally small light signal E_0 entering through mirror 1, with transmission coefficient t_1, by the time it passes through mirror 2 with transmission coefficient t_2 it has acquired an additional phase $\exp(-ik'L)$ that has both real and complex components and also incorporates the effects of optical gain at frequency ω and the distributed loss α. Describing the electric field in complex exponential notation, we can write the output wave as an infinite series of waves reflected back and forth

within the Fabry–Perot cavity while allowing for partial transmission of the wave at mirror 2, as shown in Fig. 1.3. Summing the series yields

$$E_t = E_0 t_2 t_1 e^{-ik'L}\left(1 + r_2 r_1 e^{-2ik'L} + r_2^2 r_1^2 e^{-4ik'L} + \cdots\right) = \frac{E_0 t_2 t_1 e^{-i(\tilde{k}+\Delta k)L} e^{(\gamma-\alpha)L/2}}{1 - r_2 r_1 e^{-2i(\tilde{k}+\Delta k)L} e^{(\gamma-\alpha)L}} \tag{1.14}$$

For laser oscillation to occur, it is necessary that the denominator of this equation approach zero, so that a finite output can be generated by amplification of an infinitesimally small input signal. This can happen when the denominator vanishes, leading to two conditions for oscillation, one on the threshold gain required to overcome the distributed losses in the cavity, and the other on the phase of the waves:

$$\begin{aligned} r_1 r_2 \exp\{[\gamma_{th}(\omega) - \alpha]L\} &= 1 (\text{amplitude}) \text{ and} \\ 2[k + \Delta k(\omega)]L &= 2\pi m, \quad m \text{ an integer (phase)} \end{aligned} \tag{1.15}$$

The phase condition effectively guarantees that a standing electromagnetic wave will be generated in the resonant cavity, and the amplitude condition says that the wave will grow in amplitude as long as the gain exceeds the threshold value. The mth frequency at which the cavity will oscillate can be derived from the phase condition to be:

$$[k + \Delta k(\omega)]L = kL\left[1 + \frac{\chi'(\omega)}{2n^2}\right] = m\pi \Rightarrow \omega_m = \omega\left[1 - \frac{\omega - \omega_0}{\Delta\omega}\frac{\gamma(\omega)}{k}\right] \tag{1.16}$$

If the laser resonator has a photon lifetime τ_0, we can use this to calculate the threshold population inversion as well, assuming that the population in the level N_1 is initially negligible:

$$\tau_0 = \frac{2nL}{c(1 - R_1 R_2 e^{-2\alpha L})} \approx \frac{2nL}{c[2\alpha L - \ln(R_1 R_2)]} \Rightarrow N_{2threshold} = \frac{8\pi}{A_{21}\lambda^2 g(\nu) c\tau_0} \tag{1.17}$$

In laser oscillators typical of those used in most materials-processing application, the mechanism described here results in the emission of a laser pulse that will persist until the population inversion has been extinguished, typically on a time comparable to the photon lifetime in the cavity (1.17). Figure 1.4 shows how the longitudinal modes of a Fabry–Perot cavity are modulated by the gain profile of the laser medium. Those modes on which the *net* gain exceeds the lasing threshold as defined by (1.15) will oscillate randomly; in a kind of Darwinian competition, various modes will oscillate until all are driven down to the threshold gain level.

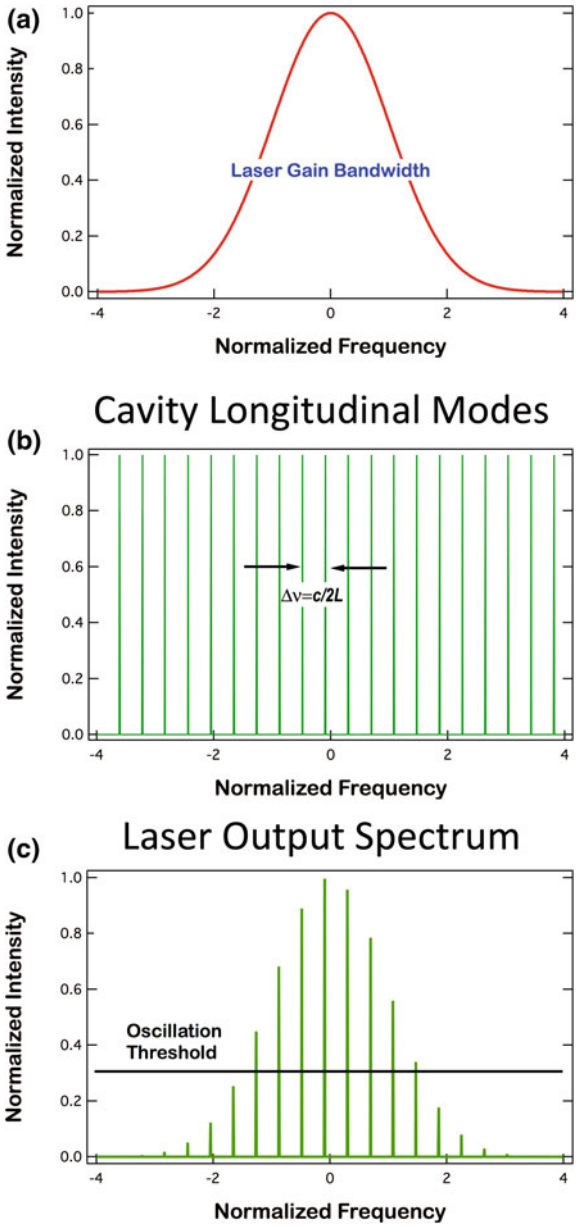

Fig. 1.4 **a** Schematic laser gain profile, derived from the atomic or molecular laser line. **b** Longitudinal cavity modes, spaced by the inverse of the cavity round-trip time. **c** Output spectrum convoluting the cavity modes with the laser gain profile; those modes that have intensity above threshold all cavity modes can lase in competition with one another

1.3.4 Mode-Locked Oscillators

Because the gain created in the excitation cycle is subject to statistical fluctuations, there may be substantial pulse-to-pulse variations in duration and energy. However, there is another approach that is designed to minimize these fluctuations, called *mode-locking*. The fundamental idea of mode-locking is the following: At a given frequency v, the gain $\gamma(v)$ satisfies

$$\gamma_{threshold}(v) = \alpha - \frac{1}{L} r_1 r_2 \Leftrightarrow \gamma(v) = (N_2 - N_1)\frac{c^2}{8\pi n^2 v^2 \tau_{spont}} g(v) \tag{1.18}$$

Moreover, we know that wherever the gain at a given frequency is sufficient to overcome the losses in the optical cavity, laser oscillations can occur over a range of frequencies v_q defined by

$$v_{q+1} - v_q = \frac{c}{2nL} \text{ or } \omega_q - \omega_{q-1} = \frac{\omega c}{L} \equiv \Omega \tag{1.19}$$

In essence, as long as there is sufficient gain, all the frequencies that differ from each other by the inverse of the round-trip propagation time in the cavity can oscillate. The total electric field at some arbitrary point in the cavity can be made periodic in the cavity round-trip time

$$E(t) = \sum_n E_n \exp[i(\omega_0 + n\Omega)t + \phi_n] = E(t+T), T = \frac{2\pi}{\Omega} = \frac{2L}{c} \tag{1.20}$$

provided that the phase ϕ_n, which normally fluctuate in a random fashion in the cavity, can be made equal to each other, that is *locked*. In this circumstance, the cavity modes E_n all have the same phase relationship with each other, and if the amplitude of all the electric field modes is constant, the total electric field is

$$E(t) = \sum_{-(N-1)/2}^{+-(N-1)/2} E_0 \exp[i(\omega_0 + n\Omega)]t = \exp\,[i\omega_0 t]\frac{\sin(N\omega t/2)}{\sin(\omega t/2)} \tag{1.21}$$

where ω_0 is the frequency at the center of the gain profile. The average oscillator output power, which is proportional to the square of the electric field, is then given by

$$P(t) \propto |E(t)|^2 = \frac{\sin^2(N\omega t/2)}{\sin^2(\omega t/2)} \tag{1.22}$$

What this means is that the power is emitted in a train of pulses separated from other by the cavity round-trip time, and where the individual pulse duration is $2L/cN$. Just as the intensity of light from N coherently interfering apertures is N^2 times the intensity from a single aperture, the power from N interfering modes is N^2 times the power from a single mode. Moreover, the pulse duration, approximated as the time from the peak to the first zero of the mode-locked train, is $1/N$ times the

round-trip time T. Estimating the number of oscillating modes as the ratio of the transition linewidth $\Delta\omega$ to the intermode frequency spacing Ω, the pulse duration τ_0 is

$$\tau_0 \sim \frac{2\pi}{\Delta\omega} = \frac{1}{\Delta\nu} \tag{1.23}$$

Hence the larger the transition linewidth for the laser transition is, the shorter is the pulse that can be obtained by mode-locking. Importantly, in solid-state laser materials, this linewidth depends not only on the lasing atom or ion, but also on the host material in which the optically active ion is embedded. In addition, since the laser is being pumped continuously, the pulse-to-pulse variation in the mode-locked train tends to be substantially smaller than in laser oscillators in which the pumping or excitation cycle produces a single output pulse.

As long as the mode-locked laser cavity is continuously excited, pulses will be generated continuously at a frequency $c/2L$, which for typical cavity dimensions of tens of centimeters leads to pulse repetition frequencies from tens of MHz to a few GHz. The energies of these pulses are usually in the nJ range and must therefore be amplified to reach the typical J/cm^2 fluences required for laser processing. However, at the very highest pulse-repetition frequencies, even the thermal loading produced by the oscillator pulses is often unacceptably high, creating a requirement either to scan the beam at high speeds so that the requirements of thermal and stress confinement are satisfied, or to reduce the pulse-repetition frequency to an acceptable level. This is generally accomplished by time-dependent modification of the resonant cavity, as will be explained below.

1.3.5 Laser Amplifiers

The majority of lasers used in materials processing are oscillators, either continuous-wave (such as diode lasers) or pulsed. However, increasingly the advantages of mode-locked oscillators—pulse durations in the femtosecond and picosecond range, and excellent power stability—are generating interest in their use in materials processing. The chief difficulty with that is the output of mode-locked oscillators comes at very high pulse-repetition frequencies, leading to undesirable thermal loading for some applications, but very low pulse energies. This leads to the need for amplification.

We assume for purposes of discussion that we are dealing with a two-level system, and that for simplicity, the amplifier medium is homogeneously broadened. Then the processes we need to deal with are: the pumping rates per unit volume into level 2 and level 1, the radiative decay from those two levels, stimulated absorption or emission on the laser transition arising from interaction with a beam of radiation, and the population of the lower level by the process of spontaneous emission. With these assumptions, it is possible to write down a pair of rate equations that describe the time evolution of these two levels.

$$\begin{aligned}\frac{dN_2}{dt} &= R_2 - N^*\sigma_{21}(\omega_L-\omega_0)\frac{1}{\hbar\omega_L} - \frac{N_2}{\tau_2}, \quad \text{where } N^* \equiv N_2 - \frac{g_2}{g_1}N_1 \\ \frac{dN_1}{dt} &= R_1 - N^*\sigma_{21}(\omega_L-\omega_0)\frac{1}{\hbar\omega_L} - \frac{N_1}{\tau_1} + N_2A_{21}\end{aligned} \tag{1.24}$$

Assuming that we are in a steady state, that is, that the lifetimes are long compared to whatever processes lead to loss of inversion, we have

$$\left.\begin{aligned}N_2 &= R_2\tau_2 - N^*\sigma_{21}\tfrac{I}{\hbar\omega_L}\tau_2 \\ N_1 &= R_1\tau_1 + N^*\sigma_{21}\tfrac{I}{\hbar\omega_L}\tau_2 + N_2A_{21}\tau_1\end{aligned}\right\} \Rightarrow N^* = \frac{R_2\tau_2[1-(g_2/g_1)A_{21}\tau_1] - (g_2/g_1)R_1\tau_1}{1+\sigma_{21}\tfrac{I}{\hbar\omega_L}[\tau_2+(g_2/g_1)\tau_1(1-A_{21}\tau_2)]} \tag{1.25}$$

Since this inversion density basically determines the magnitude of the gain and its duration, we can now notice that the numerator in the equation for N^* is the gain in the absence of the radiation field, which we denote $N^*(0)$, while the denominator contains a time-dependent term which is essentially the relaxation time for the population inversion:

$$\begin{aligned}N^*(I) &= \frac{N^*(0)}{1+\frac{I}{I_{sat}(\omega_L-\omega_0)}} \\ I_{sat}(\omega_L-\omega_0) &\equiv \frac{\hbar\omega_L}{\tau_R}\frac{1}{\sigma_{21}(\omega_L-\omega_0)}, \tau_R \equiv \tau_2 + \frac{g_2}{g_1}\tau_1[1-A_{21}\tau_2]\end{aligned} \tag{1.26}$$

The saturation intensity I_{sat} is a measure of how much the population inversion is affected by the presence of radiation in the cavity: If $I \ll I_{sat}$, the population inversion is changed very little by the intensity in the cavity; if $I \gg I_{sat}$, then the population inversion is strongly depleted by the presence of the radiation in the cavity. These (1.25) can be recast into a particularly useful form if we define a net pumping rate R^*, leading to an expression for the inversion rate per unit volume

$$\frac{dN^*}{dt} = R^* - \left(1+\frac{g_2}{g_1}\right)\frac{N^*}{\tau_R}\frac{I}{I_{sat}} + \text{spontaneous emission terms} \tag{1.27}$$

In any of the lasers commonly used in materials processing, the spontaneous emission terms are small compared to the other two terms, and can be safely neglected. Equation (1.26) essentially states that the inversion rate—which determines the gain—is proportional to the pumping rate diminished by a term that is inversely proportional to the relaxation time and directly proportional to the laser intensity in the cavity.

The practical effect of this situation for a laser amplifier is that as the intensity in the amplifier increases, the intensity gain for light traversing the amplifier in the z direction changes from exponential in the small-signal region to linear in the saturated region:

$$\frac{1}{I}\frac{dI}{dz} = \frac{\gamma_0(\omega - \omega_0)}{1 + (I/I_{sat})(\omega - \omega_0)} \Rightarrow \ln\left[\frac{I(z)}{I(0)}\right] = \gamma_0 z - \frac{I(z) - I(0)}{I_{sat}} \tag{1.28}$$

There are two limiting cases to be considered: When the intensity in the amplifier is respectively small or large compared to I_{sat}. The solutions to (1.28) in the two cases are:

$$I(z) \approx I(0)\,\exp(\gamma_0 z),\ I \ll I_{sat} \quad \text{and} \quad I(z) \approx I(0) + (\gamma_0 z) I_{sat} \tag{1.29}$$

This equation is strictly valid only for a continuous, rather than a pulsed, amplifier and for a homogeneously broadened gain medium. Nevertheless, rigorous analysis of the more complex cases of inhomogeneously broadened laser media and pulsed amplification comes to what is for all practical cases essentially the same conclusion: in the region of small signals, the gain increases exponentially with increasing distance z, while as the intensity in the amplifier rises to well above the saturation intensity, the gain is essentially linear. Plots of the two cases are shown in Fig. 1.5.

1.4 Laser Systems Used in Materials Processing

Historically, most lasers used in laser processing in industry have been oscillators; this is particularly true of lasers used in cutting, welding and similar applications, which are mostly of the continuous-wave (CW) type. However, nanosecond-pulsed, solid-state (e.g., Nd:YAG) and gas (e.g., KrF, ArF) lasers are also in widespread use. Increasingly, pulsed fiber lasers are also finding application both in research laboratories and on the factory floor. In this section, we briefly sketch the characteristics of four different types of laser oscillators to illustrate how different laser types embody the basic principles described in Sect. 1.2.

1.4.1 Laser Oscillators

Here we consider four examples of laser oscillators used in materials processing in order to illustrate the principles of laser physics from the preceding section. Further details about these specific lasers and other laser types may be found particularly in [10, 11].

Excimer lasers The rare-gas halide lasers have been part of the standard repertoire of lasers for thin-film processing since their first application in the deposition of thin films of high-temperature superconductors more than a quarter century ago. Rare-gas halide lasers—such as KrF, ArF and XeCl—are essentially two-level lasers in which the lower laser level is so weakly bound that it decays on a time scale short enough to prevent the accumulation of population in the lower

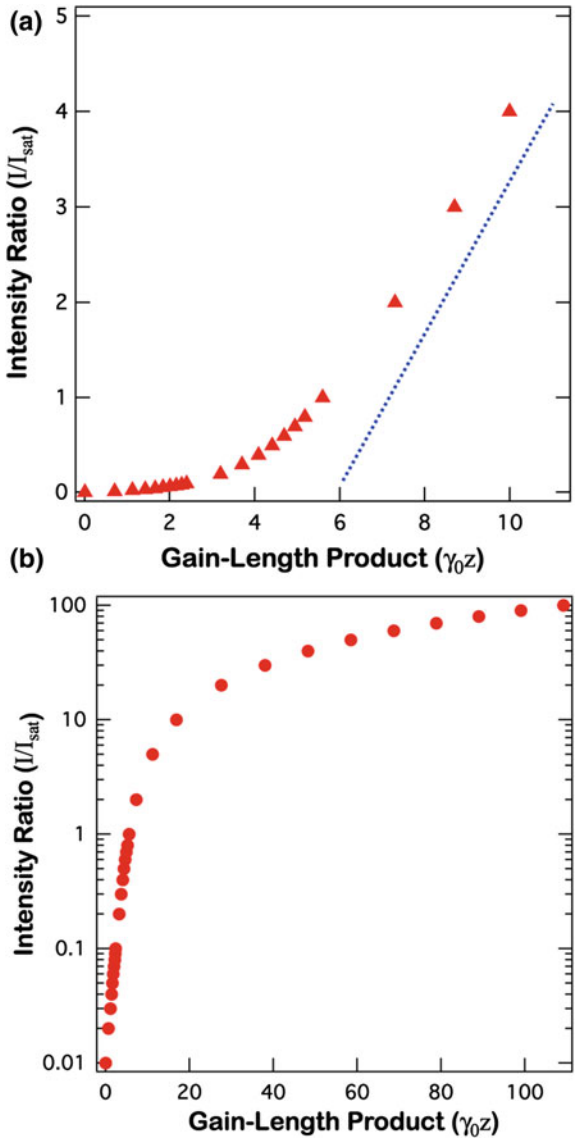

Fig. 1.5 Intensity normalized to the saturation intensity I_{sat} as a function of the gain-length product $\gamma_0 z$ in (**a**) the small-signal and (**b**) large-signal regimes

laser level [13, 14]. The energy-level diagram appropriate to this family of lasers is shown in Fig. 1.6a. The KrF laser, for example, is based on the three-body recombination reaction $Kr^+ + F^+ + Ar \rightarrow KrF^* + Ar$, where the ions may be created from the initial gas mixture by electron-beam excitation, or by preionization of the laser gas followed by an electric-field discharge. In current excimer laser designs, the preionization step seeds the discharge with 10^8–10^9 electrons—usually by a corona discharge from both sides of the laser cavity—so that the

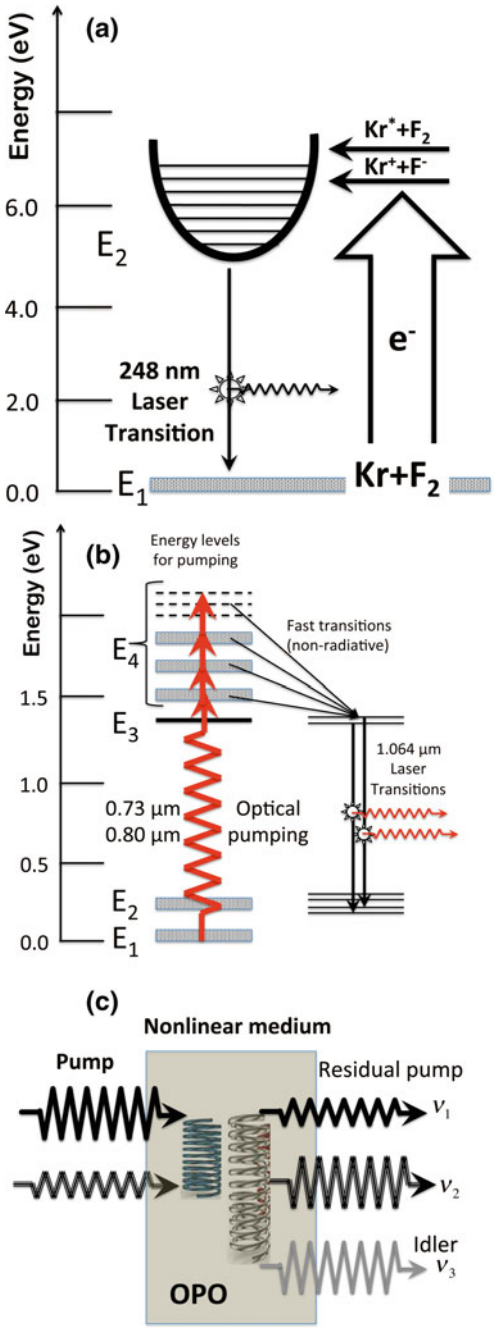

Fig. 1.6 Three different oscillator types. **a** Energy level diagram of the KrF rare-gas halide laser. **b** Energy level scheme for the Nd:YAG oscillator showing the highest gain 1.06 µm transition. **c** An optical parametric oscillator, showing the pump and seed beams, with outputs of the residual pump, signal and idler beams. The springs symbolize the wave-wave interactions in the nonlinear medium.

discharge can be homogeneous throughout the laser excitation volume; to facilitate the formation of a uniform discharge rather than plasma filaments, the gas mixture is typically 90 % He.

In a typical excimer laser, the laser cavity is bounded by plane mirrors. Since the round-trip gain is of order 100, the laser output is limited by the duration of the uniform discharge in the gain medium, typically 10–20 ns. This means, however, that the laser beam is of relatively poor quality compared to a continuous-wave laser oscillator, in which the very large number of round trips built up in the resonator tend to compress the radial mode volume and improve the output mode to the desirable and familiar TEM_{00} shape with a Gaussian radial distribution.

Nd:YAG lasers The Nd:YAG laser is one of a family of lasers that are based on laser transitions in rare-earth ions embedded in a variety of crystal hosts, including yttrium–aluminum-garnet (YAG), glass, and vanadate (YVO_4). These lasers are the classic examples of a four-level laser system as shown in the diagram in Fig. 1.6b. A recent development in multipass amplifiers has made possible a Yb:YAG laser producing over 800 W of output power in the infrared in 400 fs pulses in a compact, two-stage amplifier design [15]. One of the practical advantages of the rare-earth laser oscillators is that it is possible to generate harmonics that are often themselves intense enough for materials modification.

Optical parametric oscillators Optical parametric oscillators (OPOs) are increasingly popular as sources of moderately tunable radiation, especially for spectroscopy. However, with increasing crystal quality and output power, there is growing interest in using OPOs directly for materials research. An OPO is typically a singly- or doubly-resonant oscillator cavity in which a crystal with a large second-order susceptibility is driven by a pump beam, and possibly with a seed beam for the signal output. Well-known examples of such crystals are uniaxial, periodically poled $LiNbO_3$ or beta barium borate (BBO) pumped by a Nd:YAG laser at 1.064 or 0.532 μm wavelength. A parametric oscillator generates two output waves at the *signal* and *idler* wavelengths that simultaneously satisfy the requirements of collinear propagation and energy conservation according to:

$$\frac{n_{signal}}{\lambda_{signal}} = \frac{n_{pump}}{\lambda_{pump}} - \frac{n_{idler}}{\lambda_{idler}} \text{ and } \frac{1}{\lambda_{signal}} = \frac{1}{\lambda_{pump}} - \frac{1}{\lambda_{idler}} \tag{1.30}$$

Just as in an ordinary laser oscillator, the signal and idler wavelengths develop from random noise in the oscillator cavity that satisfies the condition for difference-frequency mixing. The input angle and cut of the nonlinear, birefringent crystal must be adjusted—typically by a combination of angle and/or temperature tuning—so that the requisite phase-matching condition between signal and idler are satisfied. While OPOs are still found primarily in analytical applications, their growing efficiency and output power/energy are leading to renewed interest in their use for laser processing [16].

Fiber lasers Fiber oscillators with output powers of a few Watts now dominate such laser-processing applications as marking. However, high-power fiber laser oscillators and large-mode-aperture systems (LMAs) are beginning to displace

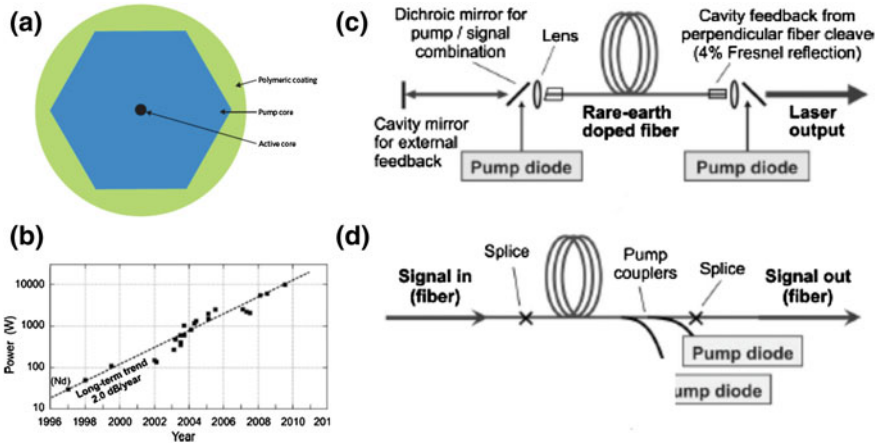

Fig. 1.7 **a** Cladding-pumped fiber geometry, from [19]. **b** Growth in fiber-laser output power as a function of year, from [17]. **c, d** Two different pumping schemes for large mode-area fiber amplifiers, also from [17]

Nd:YAG and CO_2 gas lasers that historically have been industry workhorses for high-power laser applications such as cutting and welding [17]. With powers in excess of 50 kW, these fiber lasers are much easier to incorporate into laser tools than lasers emitting free-space beams that may require complicated beam-steering optics in articulated mechanical arms to follow complex cutting or welding trajectories. Moreover, their compact construction, fundamental simplicity and durability are making it possible to use these lasers in applications for which older high-power laser types are too expensive or too complicated. While low-power fiber lasers have been under development since the 1960s and have been deployed in telecommunications applications since the 1970s, serious development of high-power fiber lasers became possible only with the discovery of the cladding-pumped fiber laser in 1988, shown schematically in Fig. 1.7a [18]. Current fiber lasers are based on a lasing transition in Yb ions in a variety of optical fibers, and emit at 1,070–1,080 nm; pumping in most cases is accomplished by 915 nm laser diodes that directly pump the $^2F_{7/2}$–$^2F_{3/2}$ transition of the Yb^{3+} ions. Output powers are now well into the multi-kW range, and growing at nearly exponential rates, as suggested by Fig. 1.7b. The most powerful fiber lasers use an oscillator-amplifier configuration; two different designs for these large mode-aperture fiber amplifiers are shown in Fig. 1.7c. Moreover, rapid progress is being made in developing fibers with lasing wavelengths in the mid-infrared; these will be powerful pumps for tunable mid-IR parametric amplifiers [19].

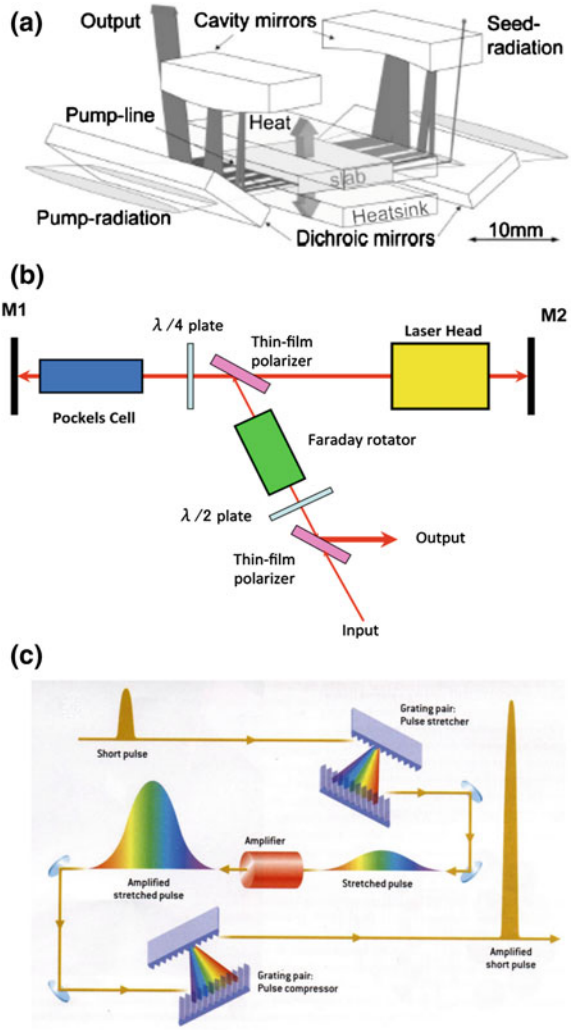

Fig. 1.8 Three different amplifier geometries: **a** the Innoslab® multipass geometry. **b** Regenerative amplifier, with a Faraday rotator to act as an optical diode. **c** the chirped-pulse amplifier, showing the stretcher grating pair, the amplifier medium and the grating-pair pulse compressor

1.4.2 Amplified Laser Systems

As pulse durations in the picosecond and femtosecond range have come into use, first as laboratory tools and more recently in a few industrial applications, master-oscillator, power-amplifier (MOPA) systems are becoming more common. The basic principles of laser gain and oscillation also apply here; however, most laser amplifier systems do not incorporate an optical cavity surrounding the gain medium. In the following paragraphs, we briefly note important characteristics of several of the most common types of laser amplifiers.

Multi-pass amplifiers One way of avoiding some of the problems of regenerative amplifiers is to use a multipass geometry like that shown in Fig. 1.8a [20]. This is in some ways a natural geometry for solid-state lasers that use cw laser diodes as a pump source, as the gain is being continually repumped, and thus is not depleted each time a pulse to be amplified passes through the gain medium. This generally requires a more complex optical arrangement and the overlap between the input or pump beam and the amplified pulses may not be as good as it is in a regenerative amplifier. While poor beam overlap may in principle lead to a loss of efficiency, in practice efficiencies of order 30 % may be achieved in multipass power amplifiers, comparable to the best regenerative devices. Moreover, the fact that amplification does not take place in an optical cavity means that problems of prepulse and amplified spontaneous emission are not a factor in multipass geometries.

Regenerative amplifiers are used to amplify laser pulses with durations ranging from femtoseconds to tens or even hundreds of picoseconds. As shown in Fig. 1.8b, amplification is carried out in an optical cavity into which the pulse to be amplified is injected, usually from a mode-locked oscillator. When the Pockels cell is off, incident laser pulses will exit the cavity via the polarizer after being reflected from the end mirror. If the Pockels cell is on because a quarter-wave voltage has been applied to it, the orthogonally polarized pulse returns to the intracavity polarizer and is trapped in the cavity, where it may make many passes through the laser gain medium. When a second quarter-wave voltage pulse is applied to the Pockels cell, the amplification cycle is ended and the amplified pulse exits the cavity. The Faraday rotator acts as an optical diode, ensuring that the amplified pulse travels only in the desired direction.

Chirped-pulse amplifiers To achieve the highest possible output intensities for femtosecond amplifiers, chirped-pulse amplifier (CPA) configurations are used, as shown schematically in Fig. 1.8c. The CPA solves the problem that amplification of a femtosecond laser pulse in a highly saturated gain medium is likely to exceed the damage threshold for the laser crystal, the laser optics, or both [21, 22]. For example, in a Ti:sapphire amplifier, the saturation fluence is of order 1 J/cm^2; hence the peak intensity of a 100 fs pulse at saturation fluence is of order 10^{13} Wcm^2—perilously close to the damage limits of most optical elements. This problem is solved in the CPA by stretching the oscillator pulse to the nanosecond regime in a dispersive medium (prism or grating pair), amplifying in one or more stages, and then temporally compressing the pulse using all-reflective dispersive media such as a diffraction grating pair. In this way, amplification takes place at moderate intensities, avoiding the optical damage issues, while high output intensity is achieved using all-reflective optics.

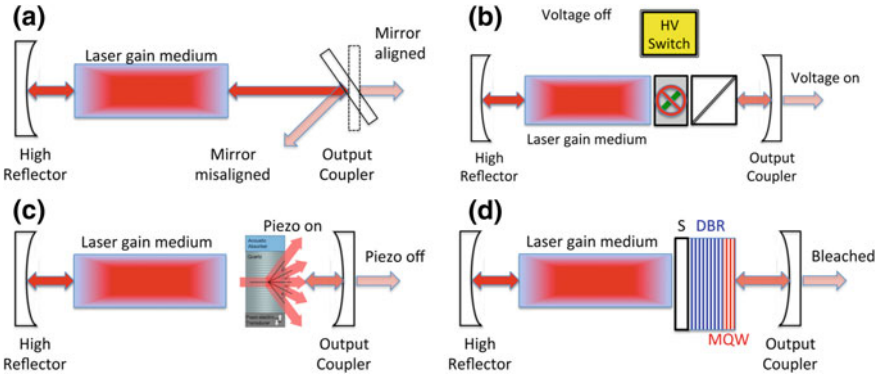

Fig. 1.9 Intracavity schemes for Q-switching. **a** Rotating mirror. **b** Electro-optic modulator. **c** Acousto-optic modulator. **d** Semiconductor saturable absorber mirror

1.4.3 Control of Laser Pulse Duration

In nanosecond and microsecond oscillators, control of the pulse generation is generally achieved by manipulating the time-dependent gain in the laser resonator, a practice often called "Q-switching" or "Q-spoiling." The idea is to allow the optical gain to be built up while not permitting oscillation, and then suddenly allowing the cavity to resonate. While the principle on which Q-switching is based is very different in concept from pulse-duration control by mode-locking, the electro-optic and acousto-optic modulators described here are also found as intracavity devices in mode-locked lasers.

The oldest of these techniques, illustrated in Fig. 1.9a, is the rotating mirror or prism. In the rotating mirror scheme, the rear high reflector in the laser cavity is rotated, so that positive feedback to the gain medium and light amplification can occur only during the brief interval of time when the output coupler and the high reflector are aligned. In between those brief intervals, the gain medium is pumped, allowing the buildup of gain far above threshold.

Electro-optic modulators make use of the Pockels effect, a second-order nonlinear effect in non-centrosymmetric crystals that allows for preferential selection of polarization in the same way that a quarter-wave plate can select for polarization. In a "Pockels cell," the polarization selectivity is created by applying a "quarter-wave voltage" that induces the necessary birefringence to block optical feedback between the high reflector and the output coupler. When the Pockels cell is turned on by applying the quarter-wave voltage, light passing through the Pockels cell converts vertically polarized light transmitted by the polarizer to circularly polarized light whose handedness is changed by reflection at the output coupler. When light can pass through the polarizer and Pockels cell with low loss, gain builds up in the cavity; horizontally polarized light is rejected by the polarizer

and exits the cavity. The beam paths are shown schematically in Fig. 1.9b. The pulse durations achieved can be as short as 2–5 ns. However, the disadvantages of this modulation scheme is the insertion of the Pockels cell into the optical cavity with its high circulating power and attendant possibility of optical damage. Moreover, the Pockels effect is relatively weak, so that achieving the desired level of birefringence requires several kV to be applied.

The *acousto-optic* modulator is an intracavity device in which the lattice planes of a piezoelectric crystal are distorted by a radio-frequency drive signal applied at one end of the crystal. When the rf power is on, the crystal planes are slightly distorted and light incident on the crystal planes, typically at near grazing angles is diffracted out of the cavity. On the other hand, when the rf power is turned off, the cavity Q is high, and lasing can occur. As with the rotating mirror, while the Q of the laser resonator is low, gain builds up as long as the laser medium is being pumped; switching from low to high gain then allows all of the gain above threshold to be extracted for as long as the rf power remains off. Given the speed of sound of a few times 10^3 m/s, a 1 mm beam will be deflected out of the cavity for a few hundred nanoseconds. This switching time can be decreased by focusing the intracavity beam inside the acousto-optic crystal. A typical arrangement is seen in Fig. 1.9c.

Saturable absorbers are materials that bleach at high intensities when all the ground-state atoms (or molecules or quantum wells) have been pumped into an excited state, precluding further absorption. If inserted into the laser cavity, a saturable absorber blocks transmission as gain is building up—thus effectively lowering the Q of the cavity—until the gain is so far above threshold that the population in the upper level of the absorber begins to saturate. As positive feedback into the cavity continues, the absorber begins to bleach until it is essentially fully transparent, and a giant, Q-switched pulse develops. Solutions of dyes and doped crystals have been widely used. In recent years, the semiconductor saturable absorber mirror (SESAM) has become increasingly popular because it is readily adapted to short cavity lengths and thus to pulse durations as short as tens of picoseconds [23]. Such an absorber is illustrated schematically in Fig. 1.9d; the saturable element is the quantum well. The advantages of the SESAM are that it is easily fabricated, has no moving parts, requires no intracavity optics, and good mode discrimination because it has a turn-on time corresponding to many cavity round trips. Since the pulse-repetition frequency of the SESAM is determined by the pump beam for the laser, it can easily operate at repetition rates up to the MHz range.

For ultrashort laser pulses, it is also possible to optimize the temporal sequence of materials processing using techniques in which a single ultrafast laser pulse is converted by opto-electronic components into a train of coherent pulses that can interact sequentially with the material to be modified [24]. In a typical pulse shaper, an ultrashort laser pulse is spatially dispersed by a diffraction grating and then passed through a spatial light modulator (SLM) that imposes a phase delay on different portions of the wavefront [25]. This SLM is often an array of liquid

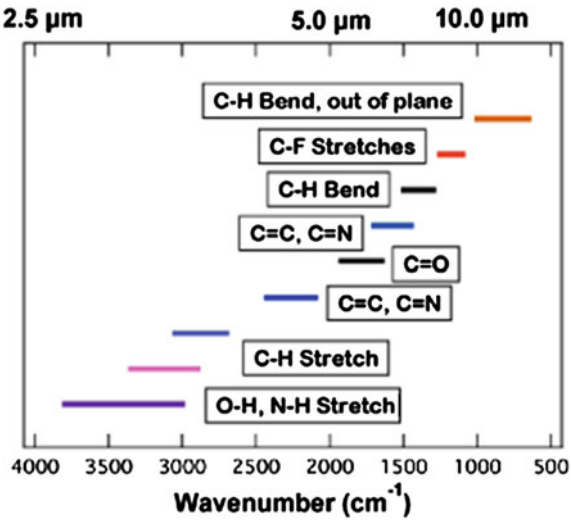

Fig. 1.10 Major vibrational bands in the "molecular fingerprint" region of the mid-infrared where polymer processing by resonant infrared excitation is possible

crystalline pixels that are individually controlled by a voltage specified via a computer. The temporal pulse sequence imposed on the input beam is then monitored by an autocorrelator or similar device. In coherent-control schemes, the SLM parameters are altered by computer control using a genetic or evolutionary algorithm based on a figure of merit that reflects the quality of the desired process outcome, such as an ion yield or a material removal rate.

1.5 A Tunable Picosecond Laser for Polymer Processing in the Mid-Infrared

To illustrate how the basic principles and systems concepts can be used to develop a novel table-top laser system for research in materials processing, we conclude by discussing a conceptual design for a table-top laser system that could replicate studies previously accomplished using an infrared free-electron laser for resonant, mid-infrared materials processing [26–28]. The system is designed to produce approximately 500 mJ/pulse at a pulse duration of 10 ps and a pulse repetition frequency of order 1 kHz; this would be adequate to reach measured thresholds for picosecond ablation of model polymers [29]. Such a system would significantly outperform the infrared free-electron laser at vastly reduced cost and complexity.

While laser processing of inorganic materials has historically been based on electronic transitions initiated by ultraviolet, visible or near-infrared lasers, processing of organic and polymer materials seems to be optimized in many cases by mid-infrared laser excitation. Most experiments in polymer or organic processing to this date have targeted O–H, C–H and N–H bands in the 3–4 μm region (see

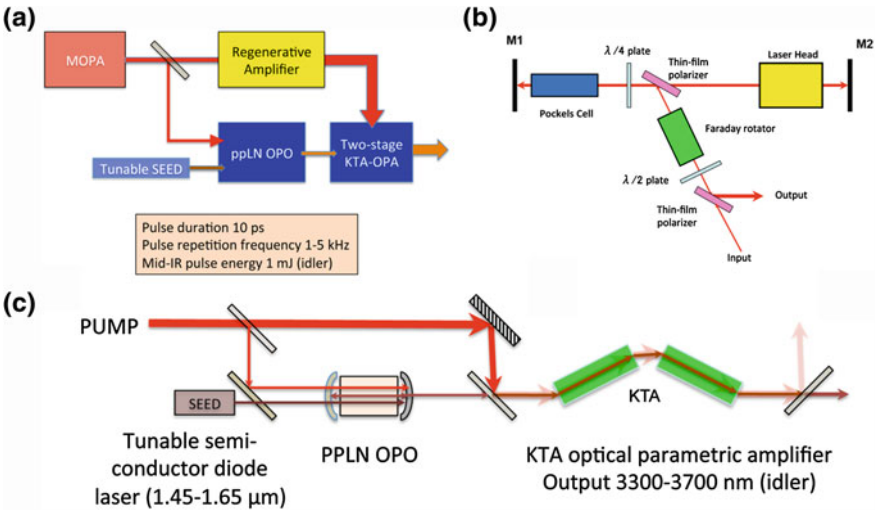

Fig. 1.11 Schematics for the ps-MIR laser system. **a** Block diagram of major system components. **b** Schematic of the regenerative amplifier. **c** Schematic of the optical parametric generator

Fig. 1.10); however, extension to other wavelength bands—such as the technologically important 5–6.5 and 8–9.5 μm stretching vibrations—with appropriate frequency-conversion elements will be highly desirable to meet laser-materials processing challenges in organic and polymer electronics and opto-electronics. In particular, developments in quasi-phase-matched frequency-conversion materials make it realistic to think about band-tunable picosecond lasers that can cover most of these absorption modes [30].

Picosecond, tunable, high-repetition lasers in the mid-infrared control the light-matter interactions selectively excite spectroscopically well-characterized vibrational states, in contrast to the multiplicity of often unknown states excited in multi- or multiple-photon *electronic* transitions. These localized, anharmonic vibrational states couple relatively slowly to the harmonic phonon bath. Mesoscale materials modifications can, in principle, be achieved by tuning the laser across the resonance to modify the local density of vibrational excitation.

It has now become possible to acquire from commercial sources all the components needed to build a tunable, mid-infrared (MIR) picosecond laser whose output is characterized by high intensity (up to 100 GW/cm^2), modest fluence (0.1–5 J/cm^2), and high pulse-repetition frequency (1–5 kHz). With these parameters and reasonable frequency-conversion efficiency, the average power in the targeted mid-infrared tuning range (2.7–3.7 μm) will need to be 10–20 W. These characteristics are sufficiently robust to enable not only proof-of-concept experiments in laser-materials interactions, but some modest scaling studies to test realistic laser-materials processing regimes at industrial scale.

Table 1.2 "Three-band" OPG output

Pump (nm)	Signal (nm)	Idler (nm)
1,064	1,670–1,690	2,872–2,932
1,064	1,520–1,540	3,442–3,560
1,064	1,450–1,470	3,852–3,996

Schematically, an example of a tunable, picosecond MIR laser is shown in Fig. 1.11a, and comprises three subsystems: the master-oscillator power-amplifier; a regenerative amplifier; and the optical parametric generator. The design is based on the successful operation of such a system used for proof-of-concept mid-infrared laser ablation and thin-film deposition experiments, first reported in 2010. We note in particular that the regenerative amplifier could be replaced by a multi-pass device; importantly, however, at pulse durations of a few picoseconds one avoids the need for chirped-pulse amplification with its added optical complexity.

The major subsystems of the ps-MIR laser are the oscillator-preamplifier (MOPA), the regenerative amplifier, and the optical parametric generator. The latter contains both the optical parametric oscillator (OPO), seeded by a tunable semiconductor diode laser, and the two-stage optical parametric amplifier for the mid-infrared generation. A collateral benefit of this design is that the pump laser can be used to provide harmonics of the Nd:YAG laser either for inorganic materials modification or for a narrow-band picosecond driver for time-resolved photoluminescence or other monitoring applications.

Based on currently available laser components, one can construct or acquire a MOPA with a linearly polarized, air-cooled fiber oscillator and high-energy fiber power amplifier. Several such MOPA systems are currently either available or under discussion for industrial applications, with typical maximum pulse energies of order 1 μJ, pulse duration of 1–10 ps and in some cases, a user-selectable pulse repetition frequency ranging from single-shot to 1 MHz. The regenerative amplifier is the most critical and most expensive component; however, the fact that the oscillator is based on a mode-locked pulse train should lead to very stable operation owing to favorable thermal (amplitude noise below ±2 %) and optical ($M^2 < 1.3$) characteristics.

The regenerative amplifier shown schematically in Fig. 1.11b could comprise one or two side-pumped Nd:YAG laser amplifier modules, and would be entirely conventional in design, differing from the typical end-pumped configuration only in the fact that the pump diodes are integral to the side-pumped modules. The amplifier module selected would need to be designed for a few tens of Watts average power.

The optical parametric generator (OPG) shown schematically in Fig. 1.11c incorporates a tunable semiconductor diode laser seeding an optical parametric oscillator (OPO) based on periodically poled lithium niobate (ppLN), and a two-stage optical parametric amplifier (OPA) using potassium tantalate (KTA) as the frequency conversion material. These robust and widely used materials produce an idler beam in the 2.8–3.8 μm range and a signal beam in the 1,450–1,690 nm band

with reasonable efficiencies. This gives adequate coverage of the O–H, N–H and C–H bands using the idler beam, and usable signal beam in the longer-wavelength telecommunications bands (Table 1.2). The OPG design is sufficiently flexible that other frequency-conversion elements could be incorporated to reach the C=C and N–N stretching vibrations (5–6.5 μm) and the fluorocarbon vibrational spectrum (8–9.5 μm). For example, quasi-phase matched GaAs could be substituted for the PPLN in the present design in order to reach even longer wavelengths [30].

1.6 Conclusion

An understanding of laser physics is the critical first step in using lasers with greatest efficiency to produced desired results in laser processing of materials. Basic considerations that relate the properties of lasers—attainable intensity and fluence, pulse duration and pulse-repetition frequency—to parameters of meso-scale and macroscale materials modifications suggest that requirements for stable, reproducible laser interactions with materials will probably lead away from many of the currently used lasers. In particular, the figure of merit suggested by (1.8) for laser processing rate clearly favors higher intensity (that is, shorter pulses) and the highest-possible pulse-repetition frequency. The versatility, growing tunability and increasing cost effectiveness of amplified, mode-locked laser systems will in all probability lead to their increasing adoption, at first in the research laboratory but inevitably in production environments.

Acknowledgments Research on infrared laser modification of materials at Vanderbilt is supported by AppliFlex LLC through a Phase II STTR grant from the National Science Foundation (IIP-0740683) and a Phase I SBIR grant from the Air Force Research Laboratories (FA9550-12-C-0006).

References

1. A.M. Stoneham, N. Itoh, Appl. Surf. Sci. **168**, 186–193 (2000)
2. N. Itoh, A.M. Stoneham, Radiat. Eff. Defects Solids **155**, 277–290 (2001)
3. L.V. Zhigilei, B.J. Garrison, J. Appl. Phys. **88**, 1281–1298 (2000)
4. L.V. Zhigilei, B.J. Garrison, Appl. Phys. Lett. **74**, 1341–1343 (1999)
5. L.V. Zhigilei, B.J. Garrison, Appl. Phy.-Mat. Sci. Proces. **69**, S75–S80 (1999)
6. L.V. Zhigilei, B.J. Garrison, Rapid Commun. Mass Spectrom. **12**, 1273–1277 (1998)
7. V.P. Carey, G. Chen, C. Grigoropoulos, M. Kaviany, A. Majumdar, Nanoscale Microscale Thermophys. Eng. **12**, 1–60 (2008)
8. E.G. Gamaly, A.V. Rode, B. Luther-Davies, J. Appl. Phys. **85**, 4213–4221 (1999)
9. A. Yariv, *Optical Electronics in Modern Communications* (Oxford University Press, New York, NY, 1997)
10. A.E. Siegman, *Lasers* (University Science Books, CA, 1986)
11. S. Hooker, C. Webb, *Laser Physics* (Oxford University Press, Oxford, 2010)
12. O. Svelto, S. Longhi, G. Della Valle, G. Huber, S. Kück, M. Pollnau, H. Hillmer, T. Kusserow, R. Engelbrecht, F. Rohlfing, J. Kaiser, R. Malz, M. Gerd, K. Mann, P. Simon,

C.K. Rhodes, F.J. Duarte, A. Borsutzky, J.A. L'huillier, M.W. Sigrist, H. Wächter, E. Saldin, E. Schneidmiller, M. Yurkov, R. Sauerbrey, J. Hein, M. Gianella, J. Helmcke, K. Midorikawa, F. Riehle, S. Steinberg, H. Brand, Lasers and Coherent Light Sources, in *Springer Handbook of Optics and Lasers*, ed. by F. Träger (Springer Verlag, Heidelberg, 2007)
13. C.A. Brau, J.J. Ewing, J. Chem. Phys. **63**, 4640–4647 (1975)
14. J.J. Ewing, C.A. Brau, Appl. Phys. Lett. **27**, 350–352 (1975)
15. P. Russbueldt, T. Mans, G. Rotarius, J. Weitenberg, H.D. Hoffmann, R. Poprawe, Opt. Express **17**, 12230–12245 (2009)
16. R.L. Byer, IEEE J. Sel. Top. Quantum Electron. **6**, 911–930 (2000)
17. D.J. Richardson, J. Nilsson, W.A. Clarkson, J. Opt. Soc. Am. B-Opt. Phy. **27**, B63–B92 (2010)
18. E. Snitzer, J. Less-Common Met. **148**, 45–58 (1989)
19. S.D. Jackson, Nat. Photonics **6**, 423–431 (2012)
20. P. Russbueldt, T. Mans, J. Weitenberg, H.D. Hoffmann, R. Poprawe, Opt. Lett. **35**, 4169–4171 (2010)
21. D. Strickland, G. Mourou, Opt. Commun. **56**, 219–221 (1985)
22. G. Mourou, D. Umstadter, Phys. Fluids B-Plasma Phys. **4**, 2315–2325 (1992)
23. U. Keller, K.J. Weingarten, F.X. Kartner, D. Kopf, B. Braun, I.D. Jung, R. Fluck, C. Honninger, N. Matuschek, J. Aus der Au, IEEE J. Sel. Top. Quantum Electron **2**, 435–453 (1996)
24. R. Stoian, A. Mermillod-Blondin, S.W. Winkler, A. Rosenfeld, I.V. Hertel, M. Spyridaki, E. Koudoumas, P. Tzanetakis, C. Fotakis, I.M. Burakov, N.M. Bulgakova, *Opt. Eng.* **44** (2005)
25. A.M. Weiner, Opt. Commun. **284**, 3669–3692 (2011)
26. M.R. Papantonakis, R.F. Haglund, Appl. Phys. A-Mater. Sci. Proces. **79**, 1687–1694 (2004)
27. S.L. Johnson, R.F. Haglund, Jr, Deposition of polymer and organic thin films using tunable, ultrafast mid-infrared lasers, in *Laser-Surface Interactions for New Materials Production: Tailoring Structure and Properties*, ed. by P. Ossi, A. Miotello (Springer Verlag, Berlin, 2009)
28. R.D. Torres, S.L. Johnson, R.F. Haglund, J. Hwang, P.L. Burn, P.H. Holloway, Crit. Rev. Solid State Mater. Sci. **36**, 16–45 (2011)
29. M. Duering, R. Haglund and B. Luther-Davies, Appl. Phys. A-Mater. Sci. Proces., doi:10.1007/s00339-013-7946-2 (2013).
30. K.L. Vodopyanov, O. Levi, P.S. Kuo, T.J. Pinguet, J.S. Harris, M.M. Fejer, B. Gerard, L. Becouarn, E. Lallier, Opt. Lett. **29**, 1912–1914 (2004)

http://www.springer.com/978-3-319-02897-2

Lasers in Materials Science

Castillejo, M.; Ossi, P.M.; Zhigilei, L. (Eds.)

2014, XVI, 387 p. 203 illus., 74 illus. in color., Hardcover
ISBN: 978-3-319-02897-2